# Ultra-small ZnO Nanodots@Functionalized Graphene Sheets from Microwave Reaction as Effective Photocatalysts

*Youjuan Zhang[1], Songtao Zhang[3], Mingbo Zheng[2,*] and Huan Pang[1,2,*]*

[1] College of Chemistry and Chemical Engineering, Anyang Normal University, Anyang, 455000, China
[2] College of Chemistry and Chemical Engineering, Yangzhou University, Yangzhou 225002, China
[3] College of Materials Science and Technology, Nanjing University of Aeronautics and Astronautics, Nanjing, Jiangsu Province, 210016, China
[*]E-mail: zhengmingbo@nju.edu.cn, huanpangchem@hotmail.com

Ultra-small ZnO nanodots@functionalized graphene sheets (ZnO@FGS) nanocomposites were synthesized by directly growing ZnO nanodots on FGS via microwave irradiation. $Zn^{2+}$ ties to FGS with oxygen-contained groups, which makes reaction start and ZnO nanodots form on FGS. The X-ray diffraction pattern reveals that wurtzite structure of ZnO is obtained. The scanning electron microscopy and transmission electron microscopy results demonstrate ZnO nanodots homogeneous dispersed on FGS. Photoluminescence spectra shows the surface defects of ZnO related emissions are quenched in the composites and the combination of graphene sheets on ZnO can apparently decrease the recombination possibility of photo-generated carries as well. The ZnO nanodots are dispersed well on FGS, which guarantees the superior optoelectronic properties of ZnO@FGS nanocomposites. Compared with ZnO, the ZnO@FGS nanocomposites show enhanced-UV photocatalytic activity for the degradation of Rhodamine B. The superior photocatalytic activity of ZnO@FGS nanocomposites is attributed to the electronic interaction between ZnO and FGS.

**Keywords:** ultra-small nanodot; ZnO; graphene; photocatalysis

## 1. INTRODUCTION

Photocatalysis is a catalytic process occurring on the surface of semiconductor materials under the irradiation of photons [1–3]. In the past few decades, many semiconductor photocatalysts have been developed for the decomposition of toxic and hazardous organic pollutants, such as $TiO_2$, $Fe_2O_3$ and ZnO, due to their unique size-dependent photoemission properties [4–6]. Especially, ZnO is one of the most promising materials because of its wide band gap (3.37 eV), large exciton binding energy (60 meV), and high electron mobility (about 115–155 $cm^{-2}$ $V^{-1}$ $S^{-1}$) [7, 8]. However, the quick

recombination of electron–hole pairs limits the use of pure ZnO for photocatalytic applications [9–11]. Many works have been devoted to reduce the recombination rate by coupling ZnO with conjugative structure carbon materials [12, 13]. In addition, in recent years, nanoparticle photocatalysts have drawn more and more attention because of their large specific surface area [14, 15]. However, nanoparticles easily aggregate, leading to difficulties in recycling and reusing. An appropriate support can efficiently prevent the aggregation of nanoparticles.

As a new carbonaceous material, graphene has attracted tremendous attention in the past years due to its large specific surface area, superior electrical conductivity, and excellent mobility of charge carriers [16–18]. The combination of semiconductors and graphene may be an ideal system to reduce the recombination rate and prevent the aggregation of nanoparticles [2, 19, 20]. It has been reported that the charge transfer between semiconductor nanoparticles and graphene sheets will greatly accelerate due to the fast diffusion of charge carries [21–23]. Several strategies have been proposed to combine graphene with ZnO nanoparticles. Li reported the incorporation of graphene with ZnO via a chemical deposition route, the significant influence of which on photocatalytic degradation of dye molecules has been investigated [24]. The incorporation of graphene greatly enhances the photocatalytic activity of the products. Zhang reported a facile, one-pot solvothermal route to grow well dispersed ZnO nanoparticles on the graphene. The effective combination and intensive interaction of ZnO with graphene improves the photocatalytic performance [25].

For the common preparation methods, the high temperature and long reaction time are inevitable. Meanwhile, the dispersion and size distribution of the semiconductor nanoparticles were usually hard to control. Microwave heating has been accepted as a promising synthesis method for nanomaterials thanks to its advantages, such as reduced energy consumption, heating the reaction mixture uniformly, shorter reaction time, and higher product yield [26–28]. In this work, we report a microwave assisted method to prepare ZnO@functionalized graphene sheets (FGS) nanocomposites. The ulra-small ZnO nanodots were uniformly distributed on FGS. Furthermore, the photocatalytic property of as-prepared composites has been investigated.

## 2. EXPERIMENTAL SECTION

### 2.1. Preparation of FGS

Graphite oxide (GO) was prepared by Hummers method [29]. To obtain FGS, certain amount of GO was thermally exfoliated at 300 °C for 5 min under air atmosphere [16].

### 2.2. Preparation of ZnO@FGS

All reagents are analytic grade and used without further purification. In a typical synthesis, 60 mg of FGS was mixed with 110 mg of $Zn(Ac)_2 \cdot 2H_2O$ in distilled water (60 mL), followed by addition of ammonia solution to adjust the pH value to around 9. Then, the suspension was placed in the microwave oven at Power of 280 W for 5 min. After cooling to room temperature, the black product

was washed and dried at 50 °C. The obtained sample was denoted as ZnO@FGS. For comparison, free ZnO nanoparticles were synthesized in the absence of FGS under the same reaction conditions.

## 2.3. Characterization

The morphology of the samples was observed by transmission electron microscopy (TEM) (JEOL JEM-2100) and scanning electron microscopy (SEM) (Gemini LEO-1530). X-ray diffraction (XRD) patterns were performed by a Bruker D8-Advance diffractometer equipped with graphite monochromatized Cu Kα, radiation (λ=0.15418 nm). The photoluminescence spectra (PL) were recorded using a Hitachi-850 fluorescence spectrometer.

## 2.4. Photocatalytic activity measurements

By selecting Rhodamine B (RhB) as the probe molecule, the photocatalytic activity evaluation was investigated using an ultraviolet lamp (30 W) as the light source. In a typical process, 10 mg of ZnO@FGS was added to 200 mL of 6 mg/L RhB aqueous solution and exposed to UV irradiation. For comparison, 4 mg of ZnO was treated under the same reaction conditions. The slurry of reaction mixture was collected and centrifuged at a speed of 8000 rpm for 5 min before the measurement by UV-vis spectroscopy. To eliminate the sorption effect of FGS, 10 mg of ZnO@FGS containing 200 mL of 6 mg/L RhB was transferred into an incubator shaker and shaken (150 rpm) in dark condition.

## 3. RESULTS AND DISCUSSION

The XRD pattern of ZnO@FGS is depicted in Fig. 1. The feature diffraction peak appearing at 23° is assigned to FGS. The remaining peaks indicate that the ZnO on FGS is of a wurtzite structure (JCPDS No. 36-1451). The average size of ZnO nanodots is about 9.0 nm according to the Debye-Scherrer formula.

The morphology characterization of FGS and ZnO@FGS is shown in Fig. 2. Fig. 2a and Fig. 2b show FGS displaying a wrinkled paper-like structure of the ultrathin graphene sheets. Both SEM image (Fig. 2c) and TEM image (Fig. 2d) of the composites indicate that ZnO nanodots are dispersed well on the graphene sheets. The high degree of dispersion of ZnO on graphene sheets guarantees the superior optoelectronic properties of ZnO@FGS.
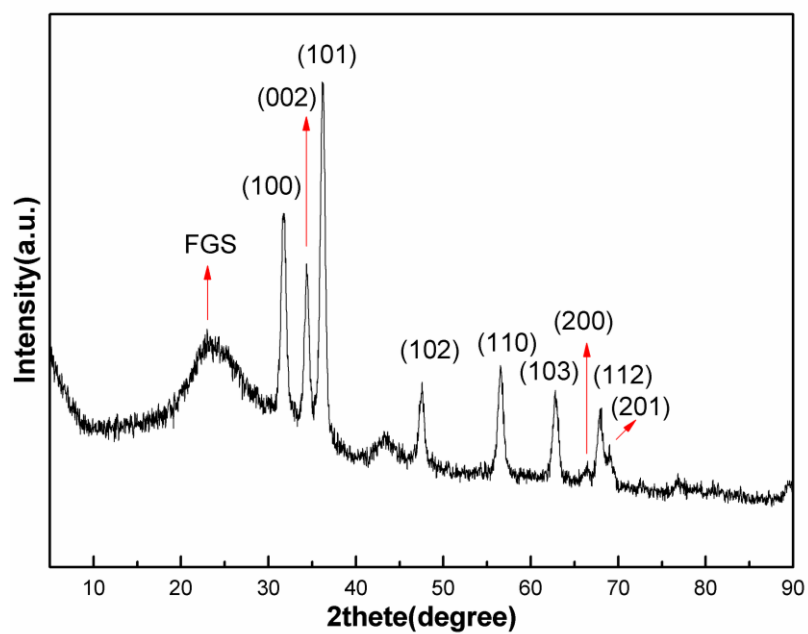
**Figure 1.** XRD pattern of ZnO@FGS.
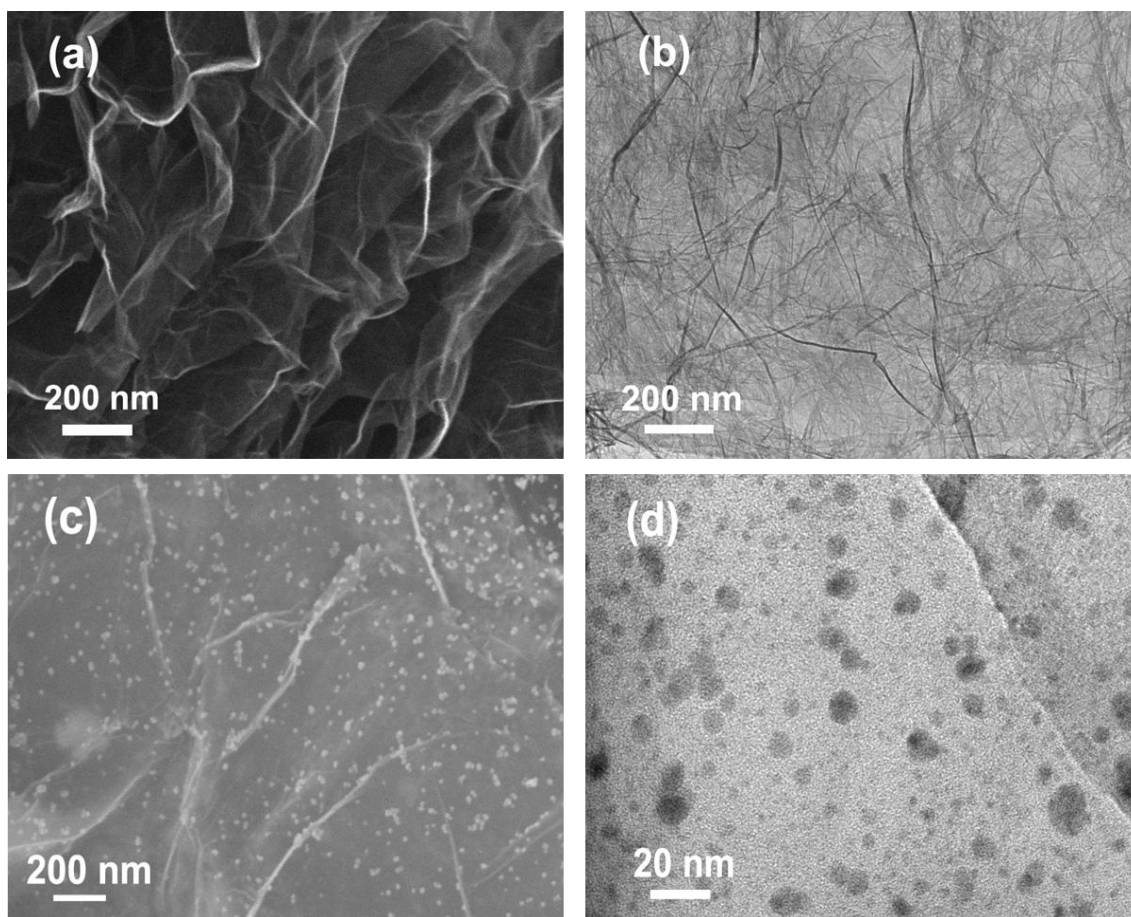


**Figure 2.** (a), (b) SEM and TEM images of FGS; (c), (d) SEM and TEM images of ZnO@FGS.
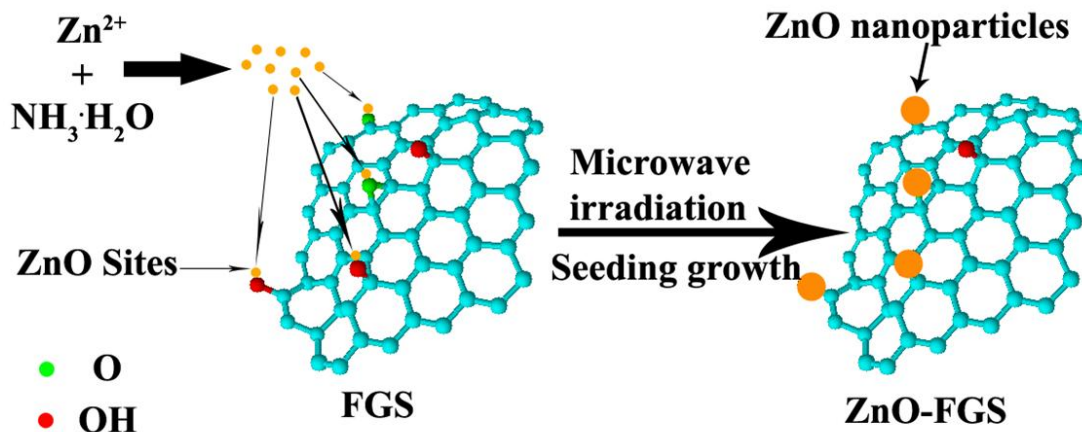
**Figure 3.** Schematic illustration of the microwave assisted synthesis of ZnO@FGS.
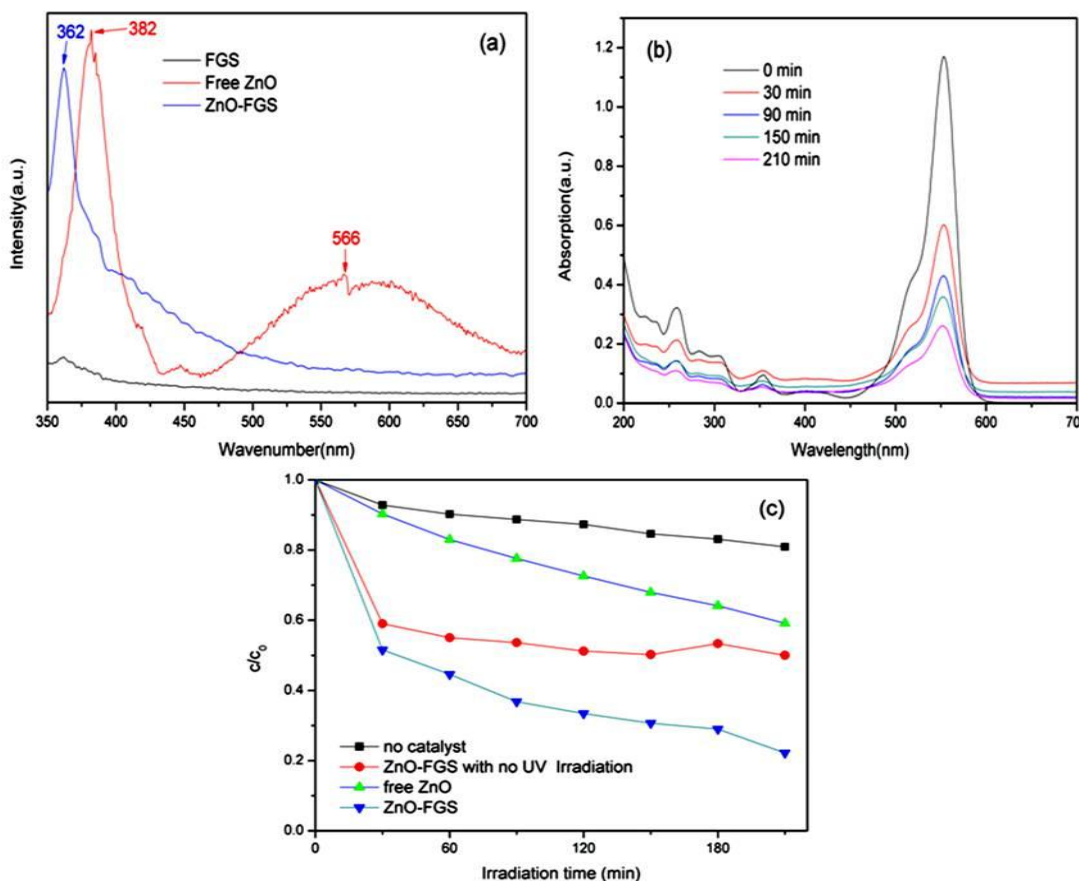


**Figure 4.** (a) The PL spectra of as-prepared samples excited at 325 nm; (b) The temporal UV–vis spectral changes of RhB aqueous solutions in the presence of ZnO@FGS at different exposure time; (c) The photocatalytic activities of different photocatalysts (including the control experiment as well) as a function of irradiation time.

The synthesis of ZnO@FGS is illustrated in Fig. 3. Our previous report indicates that FGS has many oxygen-contained groups, such as carbonyl, hydroxyl, and epoxyl groups, which make it well

dispersed in aqueous solution [16]. The $Zn^{2+}$ can anchor effectively onto FGS with oxygen-contained groups, which allows the nucleation of $Zn^{2+}$ with $OH^-$ released from ammonia solution on FGS. During the microwave heating process, ZnO nuclei formed around the sites on FGS continuously accumulate to form ZnO nanodots.

To clarify the optical property of ZnO@FGS, a study of its luminescence property was carried out. Fig. 4a shows the photoluminescence spectra of as-prepared samples at the excitation wavelength of 325 nm. The FGS is featureless in the measured region. The band edge emission of ZnO occurs at 382 nm. The secondary emission at 566 nm may be attributed to the surface defects and vacancies of the nanoparticles [8, 30]. In the spectrum of ZnO@FGS, the band edge emission of ZnO is shifted to 362 nm. The obviously blue-shifted emission of the composites indicates that the presence of quantum size effect, depending on their morphological and size variations [7, 31]. However, the emission at 566 nm is quenched due to the interaction of the surface of ZnO with FGS. This junction may suppress the recombination of photo-generated carries, which would lead to the decrease in luminescence intensity [32, 33].

We evaluated the photocatalytic performances of as-prepared samples with the photocatalytic degradation of RhB under UV irradiation. The UV-vis spectra variations of RhB (Fig. 4b) show an obvious decrease in major absorption peak at 553 nm, which demonstrates that the RhB is effectively decomposed during the photocatalysis. The concentration of RhB is determined according to the characteristic peak at around 553 nm. Fig. 4c shows the changes in the concentration of RhB with different exposure time, indicating that ZnO@FGS has greater photocatalytic activity than ZnO.

The high photocatalytic activity of composites could be attributed to the electronic interaction between ZnO and FGS, which would significantly suppress the recombination of photo-generated carries [2, 34]. The strong junction between ZnO and FGS favors charge transfer and inhibits electron-hole recombination. A high separation efficiency of electron-hole pairs and an efficient transfer of photo-generated electrons contributed to the superior electrical conductivity of FGS could enhance the photocatalytic activity [24, 33]. In addition, the conjugated RhB molecules could anchor to large aromatic domains on FGS via π-π stacking, which could facilitate reactivity performance [9].

## 4. CONCLUSION

In summary, this work demonstrated an easy microwave assisted approach to prepare ZnO@FGS nanocomposites in aqueous solution using FGS as a support. The SEM and TEM characterizations reveal homogeneous distribution of ZnO nanodots on FGS. The smooth PL spectrum of ZnO@FGS shows fewer defects than ZnO. The ZnO@FGS also show superior photocatalytic activity to ZnO. It is expected that our method could be further extended to synthesize other semiconductor nanocomposites, such as ZnS-FGS, CdS-FGS, and so on.

*Conflict of Interest*

The authors declare that they have no conflict of interest.

## References

1. TN. Lambert, CA. Chavez, B. Hernandez-Sanchez, P. Lu, NS. Bell, A. Ambrosini, T. Friedman, TJ. Boyle, DR. Wheeler and DL. Huber, *J. Phys. Chem. C*, 113 (2009) 19812.
2. IV. Lightcap, TH. Kose and PV. Kamat, *Nano Lett.*, 10 (2010) 577.
3. P. Wang, T. Jiang, C. Zhu, Y. Zhai, D. Wang and S. Dong, *Nano Res.*, 3 (2010) 794
4. J. Li, Y. Yu and L. Zhang, *Nanoscale*, 6 (2014) 8473.
5. FA. Catano, H. Gomez, EA. Dalchiele and RE. Marotti, *Int. J. Electrochem. Sci.,* 9 (2014) 534.
6. MK. Liang, MJ. Limo, A. Sola-Rabada, MJ. Roe and CC. Perry, *Chem. Mater.*, 26 (2014) 4119.
7. K. Vanheusden, WL. Warren, CH. Seager, DR. Tallant, JA. Voigt and BE. Gnade, *J. Appl. Phys.*, 79 (1996)7983.
8. P. Yang, H. Yan, S. Mao, R. Russo, J. Johnson, R. Saykally, N. Morris, J. Pham, R. He and HJ. Choi, *Adv. Funct. Mater.*, 12 (2002) 323.
9. X. Chang, G. Yu, J. Huang, Z. Li, S. Zhu, P. Yu, C. Cheng, S. Deng and G. Ji, *Catal. Today*,153 (2010)193.
10. Z. Shen, Z. Hu, W. Wang, SF. Lee, DK. Chan, Y. Li, T. Gu and CY. Jimmy, *Nanoscale*, 6 (2014) 14163.
11. Y. Zheng, L. Lin, X. Ye, F. Guo and X. Wang, *Angew Chem. Int. Ed.*, 53 (2014) 11926.
12. D. Chen, K. Wang, T. Ren, H. Ding and Y. Zhu, *Dalton Trans.*, 43 (2014)13105.
13. J. Zhang, M. Zhang, C. Yang and X. Wang, *Adv. Mater.*, 26 (2014) 4121.
14. Z. Ai, N. Wu and L. Zhang, *Catal. Today,* 224 (2014) 180.
15. S. Guo, G. Zhang, Y. Guo and CY. Jimmy, *Carbon*, 60 (2013) 437.
16. Q. Du, M. Zheng, L. Zhang, Y. Wang, J. Chen, L. Xue, W. Dai, G. Ji and J. Cao, *Electrochim. Acta*, 55 (2010) 3897.
17. Y. Liang, H. Wang, HS. Casalongue, Z. Chen and H. Dai, *Nano Res.*, 3 (2010) 701.
18. G. Williams and PV. Kamat, *Langmuir*, 25 (2009) 13869.
19. X. An, CY. Jimmy, F. Wang, C. Li and Y. Li, *Appl. Catal. B,* 129 (2013) 80.
20. PV. Kamat, *J. Phys. Chem. Lett.*, 1 (2009) 520.
21. L. Liu, X. Gu, C. Sun, H. Li, Y. Deng, F. Gao and L. Dong, *Nanoscale*, 4 (2012) 6351.
22. W. Wang, CY. Jimmy, Z. Shen, DK. Chan and T. Gu, *Chem. Commun.*, 50 (2014) 10148.
23. C. Fu, G. Zhao, H. Zhang and S. Li, *Int. J. Electrochem. Sci.*, 9 (2014) 46.
24. B. Li and H. Cao, *J. Mater. Chem.*, 21 (2011) 3346.
25. Q. Zhang, C. Tian, A. Wu, T. Tan, L. Sun, L. Wang and H. Fu, *J. Mater. Chem.*, 22 (2012) 11778.
26. HM. Hassan, V. Abdelsayed, El. Abd, SK. Rahman, KM. AbouZeid, J. Terner, MS. El-Shall, SI. Al-Resayes and AA. El-Azhary, *J. Mater. Chem.*, 19 (2009) 3832.
27. H. Wu, Q. Wang, Y. Yao, C. Qian, X. Zhang and X. Wei, *J. Phys. Chem. C*, 112 (2008) 16779.
28. S. Zhang, M. Zheng, J. Song, N. Li, H. Lu and J. Cao, *Solid State Sci.*, 38 (2014) 97.
29. WS. Hummers and RE. Offeman, *Chem. Soc.*, 80 (1958) 1339.
30. H. Wang, L. Wang, C. Qu, Y. Su, S. Yu, W. Zheng and Y. Liu, *J. Solid State Chem.*, 184 (2011) 881.

31. N. Liang, Q. He, S. Huang, M. Wang, W. Chen, M. Xu, Y. Yuan, J. Zai, N. Fang and X. Qian, *CrystEngComm*, 16 (2014) 10123.
32. D. Chen, Z. Wang, T. Ren, H. Ding, W. Yao, R. Zong and Y. Zhu, *J. Phys. Chem. C*, 118 (2014) 15300.
33. L. Qiao, X. Wang and X. Sun, *Int. J. Electrochem. Sci.,* 9 (2014) 1399.
34. T. Xu, L. Zhang, H. Cheng and Y. Zhu, *Appl. Catal. B*, 101 (2011) 382.